Author/s:
Bo, YF;Liu, YY;Soleimaninejad, H;Yu, MN;Xie, LH;Smith, TA;Ghiggino, KP;Huang, W

Title:
Photophysical Identification of Three Kinds of Low-Energy Green Band Defects in Wide-Bandgap Polyfluorenes

Date:
2019-04-04

Citation:
Bo, Y. F., Liu, Y. Y., Soleimaninejad, H., Yu, M. N., Xie, L. H., Smith, T. A., Ghiggino, K. P. & Huang, W. (2019). Photophysical Identification of Three Kinds of Low-Energy Green Band Defects in Wide-Bandgap Polyfluorenes. Journal of Physical Chemistry A, 123 (13), pp.2789-2795. https://doi.org/10.1021/acs.jpca.9b00188.

Photophysical Identification of Three Kinds of Low-Energy Green Band Defects in Wide Bandgap Polyfluorenes

Yi-Fan Bo,[a,⊥] *Yu-Yu Liu,*[a,⊥] *Hamid Soleimaninejad,*[b] *Meng-Na Yu,*[a] *Ling-Hai Xie,*[*,a] *Trevor A. Smith,*[*,c] *Kenneth P. Ghiggino,*[c] *Wei Huang*[*,a,d]

[a] Centre for Molecular Systems and Organic Devices (CMSOD), Key Laboratory for Organic Electronics and Information Displays & Jiangsu Key Laboratory for Biosensors, Institute of Advanced Materials (IAM), Jiangsu National Synergetic Innovation Center for Advanced Materials (SICAM), Nanjing University of Posts & Telecommunications, 9 Wenyuan Road, Nanjing 210023, China.

[b] Biological Optical Microscopy Platform (BOMP), Bio21 Institute Node, The University of Melbourne, Victoria 3010 Australia.

[c] ARC Centre of Excellence in Exciton Science, School of Chemistry, The University of Melbourne, Parkville, Victoria 3010, Australia.

[d] Shaanxi Institute of Flexible Electronics (SIFE), Northwestern Polytechnical University (NPU), 127 West Youyi Road, Xi'an 710072, Shaanxi, China.

[⊥] These authors contributed equally to this work.

ABSTRACT

Blue light emitting semiconductors based on polyfluorenes often exhibit an undesired green emission band. In this report, three well-defined oligofluorenes corresponding to three types of "defects" attributed to: aggregation, keto formation, and chain-entanglement, respectively, are systemically investigated to unveil the origins of the green emission band in fluorene-based materials. Firstly, the optical properties of defect molecules in different states are studied. The defect associated with aggregation is absent in the dilute solutions and in films doped at 0.01wt.% with PMMA (poly(methyl methacrylate)). Secondly, the dependence of the emission spectra as a function of solvent was monitored to compare the effects of the "keto-" and "chain-entanglement-defect" molecules. The green emission of keto defect exhibited a strong dependence on solvent polarity while that cannot be observed in chain-entanglement defect. Thirdly, energy transfer between PODPF (poly[4-(octyloxy)-9,9-diphenylfluoren-2,7-diyl]-co-[5-(octyloxy)-9,9-diphenyl-fluoren-2,7-diyl) and the keto or chain-entanglement defect molecules is illustrated. Compared with chain-entanglement defect, at low proportions of the keto defect molecule ($1:10^{-3}$), the spectra show signs of defect emission. These investigations not only provide insight into understanding the photophysics of oligofluorenes but also supply a new strategy to explore defects in semiconductor polymers, which will aid in the development of effective approaches to obtain stable pure blue OLEDs based on polyfluorenes.

1. INTRODUCTION

Polyfluorenes (PFs) are a significant class of π-conjugated materials for applications in organic light-emitting diodes (OLEDs) due to their inherent properties of pure blue emission, high luminescence quantum efficiency, good solubility and easy processability.[1-3] Moreover, PFs as host materials enable full color display through blending with other materials or via synthesis copolymers using other comonomers.[4-5] However, the undesired appearance of a low energy emission band (known as "g-band" emission) is detrimental to the lifetime stability and color purity of PFs, limiting commercial applications.[6-10] Achieving color stability and pure blue light emission with high efficiency become the most challenging goals in the field of fluorene-based polymeric light emitting diodes (PLEDs).[11] Despite intense scientific efforts to obtain stable color purity of fluorene-based OLEDs have been made,[12-14] the origin of the g-band emission is still controversial, which hinders further applications of PFs. The causes of the g-band emission are variously ascribed to "aggregation defects", the "keto defect" and the "chain-entanglement defect".[9, 15-16]

The g-band emission was initially ascribed to aggregation defects.[6] This scenario is strongly supported by the tendency toward interactions between polymer chains following the inclusion of substituents on the chain that can induce aggregation, such as hydroxy groups.[8, 17-22] In addition to the effect of molecular features, the preparation of PFs also influences the spectral properties. The fluorescence spectra of PFs in dilute THF-H_2O mixtures and in the solid state[20, 23] (especially films after annealing under nitrogen atmosphere[23]) were compared to prove the contribution of aggregation defects

to the g-band emission. In film, THF-H_2O mixtures or concentrated solution state, the influences of aggregation defects on the green emission are obvious. The molecular aggregation model has been employed to simulate[24-25] the green band emission observed from a series of experiments.

Apart from aggregation defects, it has been found that g-band emission also comes from on-chain keto defects.[26] The fluorenone groups act as energy acceptors, quenching the blue emission of PFs and initiating the g-band emission. The appearance of the green emission after annealing of PF films in air, is evidence for the contribution of keto defects to the green emission of PFs films. In addition, the fluorene-fluorenone copolymers still exhibit g-band emission even in dilute solutions providing further evidence that supports the involvement of the keto defects[27-28]. Theoretical calculations have also been performed to gain a more detailed understanding of the influence of self-trapping and non-quenching localization of excitation energy in keto defects on the green emission band[29]. Furthermore, it has been proposed that oxidation pathways that involve O_2 reacting with PFs, further confirming the keto defect mechanism.[30-32] Some of these oxidation reactions were catalyzed by residual transition metal catalysts.

Recent reports reveal that the factors behind the g-band emission are more complex and relate to other physical mechanisms.[9, 33] In 2015, Huang and Xie synthesized a hoop-shaped oligofluorene [4]CF without any keto defects that showed pure green emission in dilute solution, and proposed that a distorted conformation or entanglement of the chains of the fluorene segment may also be responsible for the g-band.[15, 34] Martin Vacha' group studied the photophysical properties of single PFO chains in different

matrices or solvents. PFO chains in the poor-solvent matrix of PMMA which expected take more compact conformations showed a larger fraction of g-band emission (58%), providing a strong support for this proposal.[35] In this paper, we use the "entanglement-chain defect" to describe the g-band emission caused by a distorted or highly strained conformation or entanglement of the chains of the fluorene segment.

And the purity of the monomers used to produce the polymer, the method of polymerization as well as the choice of catalyst are all considered as critical factors influencing the properties of the polymer. In previous investigations of the g-band emission, most of model compounds are polyfluorenes without high chemical purity and structural uniformity. One approach to overcome dispersity in an ensemble sample is to use single-molecule electroluminescence (EL) and photoluminescence (PL) spectroscopy techniques to investigate the photophysical processes related to the g-band emission in detail.[9, 35] Furthermore, the preparation of films, especially involving annealing under nitrogen atmosphere, can introduce additional discrepancies since it is difficult to eradicate the possibility of molecular structural changes, such as oxidation and decomposition, from the film. On the basis of earlier research, confirming the third origin of the g-band emission and exploring the differences among the three defect mechanisms would be profound for the design of PFs materials with stable optical properties.

Herein, to gain insight into the correlation between the origins of the g-band emission and the optical properties and molecular structures, three oligofluorenes of well-defined structures and exceptionally high levels of purity (Figure 1 for chemical structures)

involving the three different defects have been employed. 9,9,9'',9''-tetrapropyl-9H,9'H,9''H-[2,2':7',2''-terfluoren]-9'-one (TFO) is used to investigate the role of the fluorenone group in the g-band emission. Modified with hydroxy groups, 9',9''-tris(4-(octyloxy)phenyl)-9H,9'H,9''H-[2,2':7',2''-terfluorene]-9,9',9''-triol (TPFOH-3OC8) is prone to aggregation in concentrated solution and films showing green emission in their photoluminescence. Moreover, the distorted conformation or entanglement of chains in the hoop-shaped [4]cyclo-9,9-dipropyl-2,7-fluorene ([4]CF) can also induce the green emission. The optical properties of these three model molecules in dilute solutions and spin-coated films have been investigated. The relationship between energy transfer and g-band emission is also discussed.

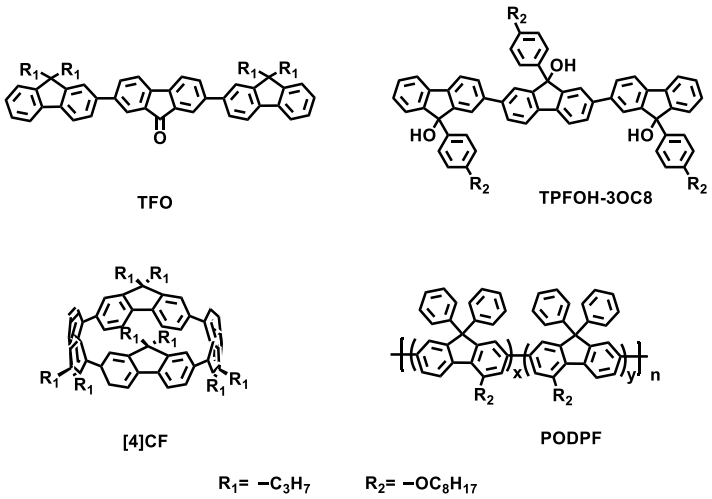

Figure 1. Molecular structures of TFO, TPFOH-3OC8, [4]CF, PODPF

2. EXPERIMENTAL SECTION

Characterization.

^{1}H NMR and ^{13}C NMR spectra were measured on a Varian Mercury Plus 400 spectrometer with tetramethylsilane as the internal standard. Ultraviolet-visible (UV-

vis) and photoluminescence (PL) spectra were measured in chloroform solution using a PerkinElmer Lambda 35 spectrophotometer and a PerkinElmer LS55 spectrophotometer, respectively. Fluorescence decay profiles were measured with a time correlated single-photon counting system that has been described previously[36], and analyzed using a standard iterative reconvolution method in the FAST (Edinburgh Instruments Ltd) software package. The absolute fluorescence quantum yield values were measured using a calibrated integrating sphere (F-3018) accessory on a Horiba FluoroLog-3 fluo-rimeter using a broadband xenon arc lamp light source.

Materials.

The synthetic pathways of the model molecules are shown in the Supporting Information (Scheme S1-2, Figure S1-3). [4]CF was synthesized according to our previous work.[15] Poly[4-(octyloxy)-9,9-diphenylfluoren-2,7-diyl]-co-[5-(octyloxy)-9,9diphenylfluoren-2,7-diyl] (PODPF, average M_n =42.7 kDa, PDI=1.6) was prepared via Yamamoto-type polymerization, according to our previous work.[37-38] To prepare the defect molecules dispersed in 0.01wt.% PMMA film, 0.01mg/mL model compounds were mixed with 1mg/ml PMMA in a microcentrifuge tube, and the mixture was homogeneously dispersed by ultrasound treatment for 30 min. The thin films of the model molecules were cast on quartz plates by spin-casting at a spin rate of 1000 rpm for 30 sec.

3. RESULTS AND DISCUSSION

The normalized steady-state UV-vis and PL spectra of the three model oligofluorenes in the film state are shown in Figure 2(a). The main absorption peaks of the three model

molecules are all around 350 nm which corresponds to the singlet π-π* transition of the fluorene backbone. In contrast to the absorption spectrum of TPFOH-3OC8 film, TFO in the film state shows a broad absorption peak from 400-500 nm corresponding to the charge transfer (CT) n-π* transition of the fluorenone segments. [4]CF in the film state has a shoulder in the absorption spectrum at 395 nm, which is attributed to the forbidden transition involving the HOMO and LUMO states based on theoretical calculations.[15] The geometry of chain-entanglement cause the structural relaxation during the process of excitation to induce the forbidden transition. Compared to the absorption spectrum of the corresponding aggregation defect molecule which exhibits only one peak, the absorption spectra of the molecules representing the entanglement chain and keto defects exhibit extra shoulder peaks or a broadened absorption band, respectively, which is a useful initial avenue to distinguish the aggregation defect from the other two defects.

The films of TPFOH-3OC8, [4]CF and TFO showed blue, green and orange photoluminescence with the peak maxima at 435 nm, 520 nm and 566 nm, respectively. A slight shoulder is also evident on the red side of the emission from TPFOH-3OC8 at approximately the same wavelength as the green emission from [4]CF (~520 nm). However, TPFOH-3OC8 in the film dispersed at 0.01 wt.% in a PMMA film exhibited pure blue emission, without any green emission band. Conversely, TFO and [4]CF dispersed at 0.01 wt.% in PMMA films still exhibited g-band emission. Similar behavior can be found for these molecules in the dilute solution state (Figure S4).

As shown in the PL spectra of [4]CF and TFO in different solvents (Figure S5-6), TFO

exhibited a strong dependence on solvent polarity whereas the emission of [4]CF is solvent independent, demonstrating the absence of specific solute-solvent interactions between the chain-entanglement defect molecules in solution.

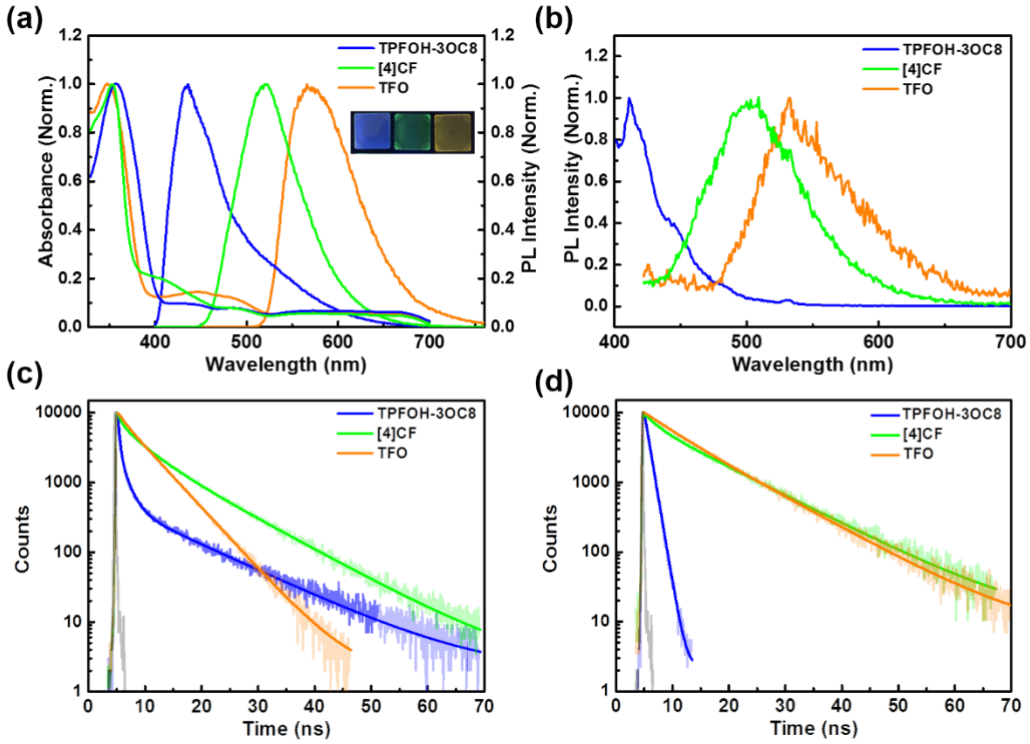

Figure 2. Absorption and PL properties of TPFOH-3OC8, [4]CF and TFO. (a) Normalized UV and PL spectra of films spin-coated from 20 mg/mL $CHCl_3$ solution. (b) PL spectra of defect molecules dispersed at 0.01wt.% in PMMA. (c) Emission decay profiles monitored in the green emission band region of films spin-coated from $CHCl_3$ (λ_{em} = 520 nm for [4]CF and TPFOH-3OC8 and 566 nm for TFO) and (d) in films at 0.01wt.% in PMMA (λ_{em} = 425 nm for TPFOH-3OC8, 500 nm for [4]CF and 540 nm for TFO).

The photoluminescence decay dynamics of the various molecules in films with and without PMMA were recorded by the TCSPC method. The emission from the pristine

films of all three model molecules, monitored at 520 nm for [4]CF and TPFOH-3OC8 and 566 nm for TFO (Figure 2 (c)), decays non-exponentially, but the decay profiles differ significantly. The best fit decay parameters of these profiles when analyzed in terms of multi-exponential decay functions are summarized in Table S1. While we do not attempt to attribute the decay times to any specific species, they have been grouped in terms of approximate decay times, $\tau_{a\text{-}e}$, in order to highlight any trends. The emission from all compounds comprises long-lived (several ns) components regardless of the origin of the emission. The keto defect (TFO) emission decay is dominated by a component of ~5 ns, with a very small contribution from a significantly shorter-lived (~1.6 ns) term. A similarly small contribution of a shorter-lived component (~0.6 ns) is also seen for the chain-entanglement defect ([4]CF) but its emission is dominated by the combination of two components; one decay term is similar to the term that dominates the TFO decay (~4 ns) and one significantly longer lived (~10 ns). The emission dynamics of the aggregation defect molecule (TPFOH-3OC8) required three or four exponential decay terms for adequate fits. When monitored at 425 nm, the emission comprises a significant contribution of a short-lived component (~0.15 ns), a second term with a decay time (~0.5 ns) similar to that seen for [4]CF, and a smaller contribution of a term with a decay time of ~2 ns. When monitored at 520 nm, the region of the shoulder in the emission spectrum overlapping with the peak of the [4]CF emission, the PL decay is dominated by an additional, long-lived (~13 ns) component. The general trend from these data is that the amplitude average lifetimes of all three compounds are significantly longer when measured at 520 nm compared to TPFOH-

3OC8 at 425 nm. The emission of both [4]CF and TPFOH-3OC8 contains the very long-lived component, suggesting that the shoulder in the TPFOH-3OC8 spectrum is due to the similar species as the green band of the [4]CF, but this is absent from the orange emission of TFO. The fluorescence quantum yields change approximately in proportion with the average emission decay times.

The decay dynamics of the various molecules dispersed at 0.01wt.% in PMMA were also investigated (Figure 2 (d)). The emission spectrum of the aggregation defect molecule (TPFOH-3OC8) doped 0.01wt.% in a PMMA film exhibited pure blue emission without any green emission. This blue emission decayed exponentially, having a decay time that was the same order of magnitude as the average lifetime observed in the corresponding pristine film monitored at 425 nm. These results strongly suggest that the longer-lived green (520 nm) emission observed in the TPFOH-3OC8 pristine film was induced by the aggregation defect. In the PMMA blend films, [4]CF and TFO both show significant emission in the green (~500-550 nm) that decays biexponentially, dominated (>85%) by a long-lived (~10 ns) component that is comparable to the component seen in the pristine [4]CF and TPFOH-3OC8 films.

Energy transfer between PODPF and the defect molecules

The presence of aggregation, keto and/or chain entanglement defects in the sample of PODPF might be expected to quench the stable, pure blue emission otherwise exhibited by films of the polymer. To further investigate the differences between the keto and chain-entanglement defects, the photophysical behaviors of the various molecules after blending with PODPF have been studied.[37-38] The emission spectra of the TFO and

[4]CF films as a function of PODPF:compound mass ratio are shown in Figure 3 and Figure S7-8. The pure blue emission of PODPF is observed at low proportions of the defect molecules, but the spectra become mixed and then dominated by emission characteristic of the corresponding defects as the PODPF:compound ratio decreases, without any blue emission at the 1:1 ratio. Even at low proportions of the keto defect molecule (PODPF:TFO ratio of $1:10^{-3}$), the spectrum shows signs of defect emission and the $1:10^{-2}$ film exhibits yellow emission under 365 nm UV lamp irradiation (Figures S9 and 3(a)). Despite the keto peak at 1712 cm^{-1}, assigned to the stretching vibration of the carbonyl species, is difficult to be observed at this ratio in the Fourier Transform Infrared (FTIR) spectra of TFO doped PODPF in KBr films (Figures S10-11). At ratios between $1:10^{-3}$ and 1:1, the PODPF:TFO films exhibit dual (blue and orange) emission. Comparatively little g-band emission is seen in the PODPF:chain-entanglement defect ([4]CF) film until the [4]CF proportion exceeds ~$1:10^{-2}$. These emission spectral changes with increasing PODPF content infers the occurrence of energy transfer in the two systems due to the overlap of the defect molecules' absorption and the PODPF emission spectra. In the case of the PODPF: keto defect molecule (TFO) system, the photoluminescence excitation (PLE) spectra monitored at 566 nm (Figure S12) show that absorption by PODPF contributes partly to the emission at 566 nm (g-band) in the film PODPF:compound ratio range of $1:1 \rightarrow 1:10^{-2}$, verifying the existence of energy transfer in the keto defect PODPF system. This method could not be applied to the PODPF:[4]CF system due to the overlap of the absorption spectra of [4]CF and PODPF. However, energy transfer in both the PODPF:[4]CF and PODPF:TFO systems can be

verified in the following time-resolved emission experiments.

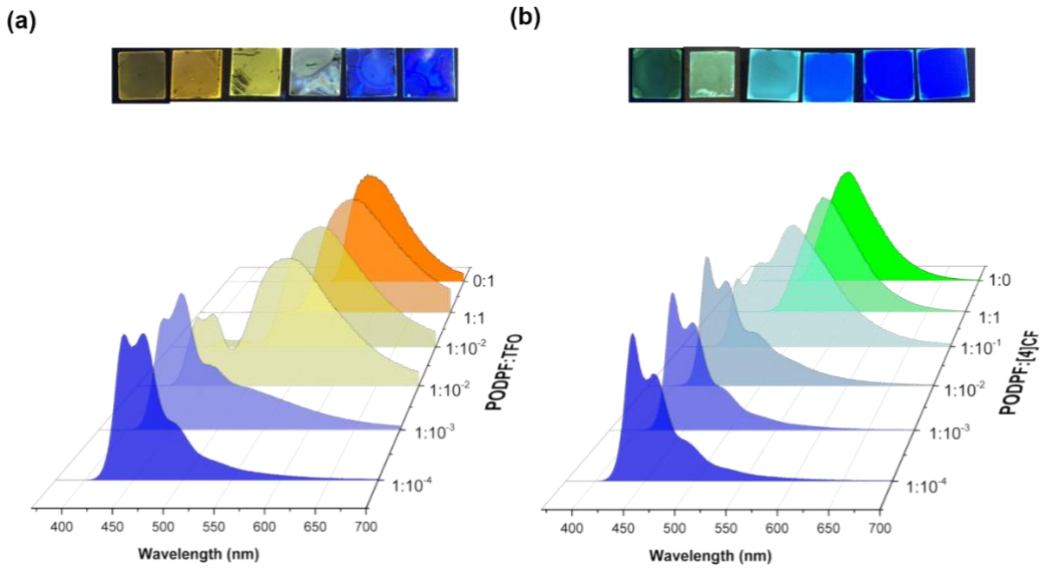

Figure 3. Normalized emission spectra of (a) TFO and (b) [4]CF doped with PODPF films at different mass ratios (λ_{ex} = 360 nm), and photographs above the spectra are films under 365 nm UV lamp irradiation (from left to right: PODPF:defect molecule=1:0, 1:1, 1:10^{-1}, 1:10^{-2}, 1:10^{-3}, 1:10^{-4}).

TCSPC measurements were carried out on samples of varying PODPF:defect molecule ratios (from 1:0 to 1:10^{-2}) (Figure 4). The decay profiles for all the films were again multi-exponential (fitting results summarized in Table S2). The emission from PODPF itself also decays multi-exponentially but is dominated by a component with a decay time of ~230 ps. A minor contribution from a longer-lived component (~3.3 ns) is evident in the PODPF emission, leading to an average fluorescence "lifetime" of ~350 ps. In the case of PODPF:TFO, the emission decays can be analyzed globally with the PODPF emission reduced to the timescale of the instrument response function at all three blend ratios and a common, extremely minor contribution of the ~3.3 ns component observed for PODPF remaining, particularly evident for the 1:1 ratio sample.

In the case of PODPF:[4]CF, the decays are complicated, since the excitation wavelength used (360 nm) could photo-excite both PODPF and [4]CF. The decays could be analyzed globally as sums of up to four exponential terms including decay components that vary (~3.5 - 5.3 ns), but are longer than the PODPF sample (~3.2 ns), however, the general trend is apparent. A large proportion of the PODPF emission is again quenched in all three samples; at 1:10 $^{-2}$ the emission is quenched significantly, but for the 1:1 and 1:10^{-1} PODPF:[4]CF samples the emission is reduced to beyond the time-resolution of the measurement.

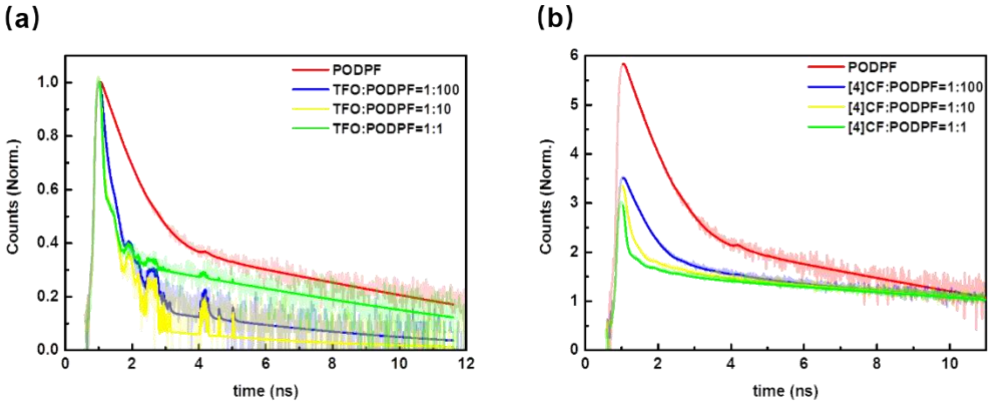

Figure 4. PL decay profiles of TFO (a) and [4]CF (b) doped with various concentrations of PODPF in the film (λ_{ex}=360 nm, λ_{em}=440 nm).

To gain further insight into the dynamics of energy transfer from PODPF to the defect molecules, we have calculated the Förster critical energy transfer radius (R) using equation (1).

$$R_0^6 = \frac{9000(\ln 10 k^2 Q_D)}{128\pi^5 N n^4} \int_0^\infty F_D(\lambda)\, \varepsilon_A(\lambda) \lambda^4 \mathrm{d}\lambda \qquad (1)$$

where Q_D is the quantum yield of the donor in the absence of acceptor (0.422), n is refractive index of the medium (n = 1.73 for Poly(9,9-dioctyl fluorene) (PFO) which is

similar to PODPF), κ^2 is usually assumed to be equal to 2/3 assuming a random distribution of orientations between the donor emission and acceptor absorption transition dipoles, $\varepsilon_A(\lambda)$ is the extinction coefficient of the acceptor at λ and $F_D(\lambda)$ is the corrected fluorescence intensity of the donor at λ. The Förster energy transfer radii (R) of [4]CF and TFO doping in the PODPF film were calculated to be 35.46 Å and 31.61 Å respectively. The efficiency of Förster energy transfer from a polymer energy donor to a lower energy acceptor can often be calculated using the emission decay times for the polymer of the energy donor in the presence and absence of the acceptor. [39-40] However, in the present case the multi-exponential nature of the decays and the reduction of the shorter decay components in the presence of the defect molecules to beyond the time resolution of the measurement make such calculations unfruitful.

The magnitude of the calculated distances and the drastic reduction in the timescale of the PODPF blue emission, particularly in the case of TFO (Figure 4), indicates that a significant number of these defects resides within 40 Å of the photoexcited PODPF chromophore, or the excitation energy can migrate efficiently until it is in the presence of a defect.

These results confirm the existence of energy transfer from PODPF to both the keto and entanglement defects in polyfluorenes, which lead to increased g-band emission.

The prevalence of these defects must therefore be reduced or controlled in order to optimize the blue emission of PODPF polymer films in practical applications.

4. CONCLUSIONS

Well-defined oligomers corresponding to three different defects were employed as

models to investigate the origins of the g-band emission in polyfluorenes. After being dissolved in solution or diluted in PMMA film, the g-band emission caused by the aggregation defect disappears. Compared with the chain-entanglement defect molecule, the emission of the keto defect molecule is dependent on the solvent polarity. To further differentiate the keto defect and chain-entanglement defect, a series of mixed PODPF/defect molecule films at different mass ratios were investigated. Energy transfer from the PODPF to the keto and chain entanglement defects was clearly observed illustrating the impact of the defects on the emission characteristics of PODPF films. The origin of g-band in polyfluorenes remains controversial. The results indicated aggregation defect, keto defect as well as chain-entanglement defect would result in g-band. The g-band of polyfluorenes is likely to result from a combination of two or three defects. In this paper, keto defect has a great significance on g-band which will affect the PL spectra in the concentration of $1:10^{-3}$(PODPF: defect molecule). Chain-entanglement defect requires relatively weak influences on g-band. The contribution of aggregation defect is not excluded here, these would also constitute a major part of the g-band.

ASSOCIATED CONTENT

Supporting Information. The synthesis route and structural characterization of TPFOH-3OC8 and TFO; Basic photophysical properties of TPFOH-3OC8, [4]CF and TFO in DCM; FT-IR spectra of TFO in bulk KBr film; summary of results obtained from multi-exponential analysis of the fluorescence decays of the model molecules

AUTHOR INFORMATION

Corresponding Author

*E-mail: trevoras@unimelb.edu.au; iamlhxie@njupt.edu.cn; wei-huang@njtech.edu.cn

Notes

The authors declare no competing financial interest

ACKNOWLEDGMENTS

The project was supported by the National Natural Science Foundation of China (21503114, 21602111, 61605090), Doctoral Fund of Ministry of Education of China (20133223110007), Natural Science Foundation of Jiangsu Province of China (BK20150832, BK20180751), The Nanjing University of Post and Telecommunications (NY217082), Synergetic Innovation Center for Organic Electronics and Information Displays and Excellent science and technology innovation team of Jiangsu Higher Education Institutions (2013). Project was funded by the Priority Academic Program Development of Jiangsu Higher Education Institutions. We also acknowledge support of the University of Melbourne IRRTF Scheme and the ARC Centre of Excellence in Exciton Science (CE170100026) (TAS).

REFERENCES

1. Xie, L. H.; Yin, C. R.; Lai, W. Y.; Fan, Q. L.; Huang, W., Polyfluorene-Based Semiconductors Combined with Various Periodic Table Elements for Organic Electronics. *Prog. Polym. Sci.* **2012**, *37*, 1192-1264.

2. Scherf, U.; List, E. J. W., Semiconducting Polyfluorenes-Towards Reliable

Structure-Property Relationships. *Adv. Mater.* **2002**, *14*, 477-487.

3. Knaapila, M.; Monkman, A. P., Methods for Controlling Structure and Photophysical Properties in Polyfluorene Solutions and Gels. *Adv. Mater.* **2013**, *25*, 1090-1108.

4. Ego, C.; Marsitzky, D.; Becker, S.; Zhang, J.; Grimsdale, A. C.; Mullen, K.; MacKenzie, J. D.; Silva, C.; Friend, R. H., Attaching Perylene Dyes to Polyfluorene: Three Simple, Efficient Methods for Facile Color Tuning of Light-Emitting Polymers. *J. Am. Chem. Soc.* **2003**, *125*, 437-443.

5. Gong, X.; Ostrowski, J. C.; Bazan, G. C.; Moses, D.; Heeger, A. J.; Liu, M. S.; Jen, A. K. Y., Electrophosphorescence from a Conjugated Copolymer Doped with an Iridium Complex: High Brightness and Improved Operational Stability. *Adv. Mater.* **2003**, *15*, 45-49.

6. Lemmer, U.; Heun, S.; Mahrt, R. F.; Scherf, U.; Hopmeier, M.; Siegner, U.; Gobel, E. O.; Mullen, K.; Bassler, H., Aggregate Fluorescence in Conjugated Polymers. *Chem. Phy. Lett.* **1995**, *240*, 373-378.

7. Koizumi, Y.; Seki, S.; Tsukuda, S.; Sakamoto, S.; Tagawa, S., Self-Condensed Nanoparticles of Oligofluorenes with Water-Soluble Side Chains. *J. Am. Chem. Soc.* **2006**, *128*, 9036-9037.

8. Chen, X.; Tseng, H. E.; Liao, J. L.; Chen, S. A., Green Emission from End-Group-Enhanced Aggregation in Polydioctylfluorene. *J. Phys. Chem. B* **2005**, *109*, 17496-17502.

9. Honmou, Y.; Hirata, S.; Komiyama, H.; Hiyoshi, J.; Kawauchi, S.; Iyoda, T.; Vacha,

M., Single-Molecule Electroluminescence and Photoluminescence of Polyfluorene Unveils the Photophysics Behind the Green Emission Band. *Nat. Commun.* **2014**, *5*, 4666.

10. Becker, K.; Lupton, J. M.; Feldmann, J.; Nehls, B. S.; Galbrecht, F.; Gao, D. Q.; Scherf, U., On-Chain Fluorenone Defect Emission from Single Polyfluorene Molecules in the Absence of Intermolecular Interactions. *Adv. Funct. Mater.* **2006**, *16*, 364-370.

11. Gross, M.; Muller, D. C.; Nothofer, H. G.; Scherf, U.; Neher, D.; Brauchle, C.; Meerholz, K., Improving the Performance of Doped π-Conjugated Polymers for Use in Organic Light-Emitting Diodes. *Nature* **2000**, *405*, 661-665.

12. Li, C.; Bo, Z., Three-Dimensional Conjugated Macromolecules as Light-Emitting Materials. *Polymer* **2010**, *51*, 4273-4294.

13. Jiang, Z.; Liu, Z.; Yang, C.; Zhong, C.; Qin, J.; Yu, G.; Liu, Y., Multifunctional Fluorene-Based Oligomers with Novel Spiro-Annulated Triarylamine: Efficient, Stable Deep-Blue Electroluminescence, Good Hole Injection, and Transporting Materials with Very Hightg. *Adv. Funct. Mater.* **2009**, *19*, 3987-3995.

14. Cocherel, N.; Poriel, C.; Rault-Berthelot, J.; Barriere, F.; Audebrand, N.; Slawin, A. M.; Vignau, L., New 3pi-2spiro Ladder-Type Phenylene Materials: Synthesis, Physicochemical Properties and Applications in OLEDs. *Chemistry* **2008**, *14*, 11328-11342.

15. Liu, Y. Y.; Lin, J. Y.; Bo, Y. F.; Xie, L. H.; Yi, M. D.; Zhang, X. W.; Zhang, H. M.; Loh, T. P.; Huang, W., Synthesis and Crystal Structure of Highly Strained [4]Cyclofluorene: Green-Emitting Fluorophore. *Org. Lett.* **2016**, *18*, 172-175.

16. Chan, K. L.; Sims, M.; Pascu, S. I.; Ariu, M.; Holmes, A. B.; Bradley, D. D. C., Understanding the Nature of the States Responsible for the Green Emission in Oxidized Poly(9,9-Dialkylfluorene)s: Photophysics and Structural Studies of Linear Dialkylfluorene/Fluorenone Model Compounds. *Adv. Funct. Mater.* **2009**, *19*, 2147-2154.

17. Pei, Q. B.; Yang, Y., Efficient Photoluminescence and Electroluminescence from a Soluble Polyfluorene. *J. Am. Chem. Soc.* **1996**, *118*, 7416-7417.

18. Pei, J.; Liu, X. L.; Chen, Z. K.; Zhang, X. H.; Lai, Y. H.; Huang, W., First Hydrogen-Bonding-Induced Self-Assembled Aggregates of a Polyfluorene Derivative. *Macromolecules* **2003**, *36*, 323-327.

19. Lu, H. H.; Liu, C. Y.; Jen, T. H.; Liao, J. L.; Tseng, H. E.; Huang, C. W.; Hung, M. C.; Chen, S. A., Excimer Formation by Electric Field Induction and Side Chain Motion Assistance in Polyfluorenes. *Macromolecules* **2005**, *38*, 10829-10835.

20. Koizumi, Y.; Seki, S.; Tsukuda, S.; Sakamoto, S.; Tagawa, S., Self-Condensed Nanoparticles of Oligofluorenes with Water-Soluble Side Chains. *J. Am. Chem. Soc.* **2006**, *128*, 9036-9037.

21. Tapia, M. J.; Burrows, H. D.; Knaapila, M.; Monkman, A. P.; Arroyo, A.; Pradhan, S.; Scherf, U.; Pinazo, A.; Perez, L.; Moran, C., Interaction Between the Conjugated Polyelectrolyte Poly{1,4-Phenylene[9,9-Bis(4-Phenoxybutylsulfonate)]Fluorene-2,7-Diyl} Copolymer and the Lecithin Mimic 1-O-(L-Arginyl)-2,3-O-Dilauroyl-Sn-Glycerol in Aqueous Solution. *Langmuir* **2006**, *22*, 10170-10174.

22. Zhu, L.; Qin, J.; Yang, C., Synthesis, Photophysical Properties, and Self-Assembly

Behavior of Amphiphilic Polyfluorene: Unique Dual Fluorescence and Its Application as a Fluorescent Probe for the Mercury Ion. *J. Phys. Chem. B* **2010**, *114*, 14884-14889.

23. Kreyenschmidt, M.; Klaerner, G.; Fuhrer, T.; Ashenhurst, J.; Karg, S.; Chen, W. D.; Lee, V. Y.; Scott, J. C.; Miller, R. D., Thermally Stable Blue-Light-Emitting Copolymers of Poly(Alkylfluorene). *Macromolecules* **1998**, *31*, 1099-1103.

24. Surin, M.; Hennebicq, E.; Ego, C.; Marsitzky, D.; Grimsdale, A. C.; Mullen, K.; Bredas, J. L.; Lazzaroni, R.; Leclere, P., Correlation between the Microscopic Morphology and the Solid-State Photoluminescence Properties in Fluorene-Based Polymers and Copolymers. *Chem. Mater.* **2004**, *16*, 994-1001.

25. M. Surin; P. Sonar; A. C. Grimsdale; K. Müllen; R. Lazzaroni; Leclère, P., Supramolecular Organization in Fluorene/Indenofluorene-Oligothiophene Alternating Conjugated Copolymers. *Adv. Funct. Mater.* **2005**, *15*, 1426-1434.

26. Lee, J. I.; Klaerner, G.; Miller, R. D., Oxidative Stability and Its Effect on the Photoluminescence of Poly(Fluorene) Derivatives: End Group Effects. *Chem. Mater.* **1999**, *11*, 1083-1088.

27. Gong, X. O.; Iyer, P. K.; Moses, D.; Bazan, G. C.; Heeger, A. J.; Xiao, S. S., Stabilized Blue Emission from Polyfluorene-Based Light-Emitting Diodes: Elimination of Fluorenone Defects. *Adv. Funct. Mater.* **2003**, *13*, 325-330.

28. Kulkarni, A. P.; Kong, X. X.; Jenekhe, S. A., Fluorenone-Containing Polyfluorenes and Oligofluorenes: Photophysics, Origin of the Green Emission and Efficient Green Electroluminescence. *J. Phys. Chem. B* **2004**, *108*, 8689-8701.

29. Zojer, E.; Pogantsch, A.; Hennebicq, E.; Beljonne, D.; Brédas, J.-L.; Scandiucci de

Freitas, P.; Scherf, U.; List, E. J. W., Green Emission from Poly(Fluorene)s: The Role of Oxidation. *J. Chem. Phys.* **2002**, *117*, 6794.

30. Sims, M.; Bradley, D. D. C.; Ariu, M.; Koeberg, M.; Asimakis, A.; Grell, M.; Lidzey, D. G., Understanding the Origin of the 535 Nm Emission Band in Oxidized Poly(9,9-Dioctylfluorene): The Essential Role of Inter-Chain/Inter-Segment Interactions. *Adv. Funct. Mater.* **2004**, *14*, 765-781.

31. Gamerith, S.; Gadermaier, C.; Scherf, U.; List, E. J. W., Emission Properties of Pristine and Oxidatively Degraded Polyfluorene Type Polymers. *Phys. Status Solidi A* **2004**, *201*, 1132-1151.

32. Liu, L.; Yang, B.; Zhang, H.; Tang, S.; Xie, Z.; Wang, H.; Wang, Z.; Lu, P.; Ma, Y., Role of Tetrakis(Triphenylphosphine)Palladium(0) in the Degradation and Optical Properties of Fluorene-Based Compounds. *J. Phys. Chem. C* **2008**, *112*, 10273-10278.

33. Farcas, A.; Assaf, K. I.; Resmerita, A. M.; Cantin, S.; Balan, M.; Aubert, P. H.; Nau, W. M., Cucurbit[7]Uril-Based Fluorene Polyrotaxanes. *Eur. Polym. J.* **2016**, *83*, 256-264.

34. Lin, Z. Q.; Shi, N. E.; Li, Y. B.; Qiu, D.; Zhang, L.; Lin, J. Y.; Zhao, J. F.; Wang, C.; Xie, L. H.; Huang, W., Preparation and Characterization of Polyfluorene-Based Supramolecular π-Conjugated Polymer Gels. *J. Phys. Chem. C* **2011**, *115*, 4418-4424.

35. Nakamura, T.; Sharma, D. K.; Hirata, S.; Vacha, M., Intrachain Aggregates as the Origin of Green Emission in Polyfluorene Studied on Ensemble and Single-Chain Level. *J. Phys. Chem. C* **2018**, *122*, 8137-8146.

36. Motyka, M.; Steer, R. P.; Williams, C. C.; Lee, S.; Ghiggino, K. P., Concerning the

Dual Emission of Porphyrazines Employed in Biomedical Imaging. *Photochem. Photobiol.* **2013**, *12*, 1086-1090.

37. Lin, J. Y.; Zhu, W. S.; Liu, F.; Xie, L. H.; Zhang, L.; Xia, R.; Xing, G. C.; Huang, W., A Rational Molecular Design of *β*-Phase Polydiarylfluorenes: Synthesis, Morphology, and Organic Lasers. *Macromolecules* **2014**, *47*, 1001-1007.

38. Liu, B.; Lin, J. Y.; Liu, F.; Yu, M. N.; Zhang, X.; Xia, R. D.; Yang, T.; Fang, Y.; Xie, L. H.; Huang, W., A Highly Crystalline and Wide-Bandgap Polydiarylfluorene with *β*-Phase Conformation Toward Stable Electroluminescence and Dual Amplified Spontaneous Emission. *ACS Appl. Mater. Interfaces* **2016**, *8*, 21648-21655.

39. Bi, P.; Zheng, F.; Yang, X.; Niu, M.; Feng, L.; Qin, W.; Hao, X., Dual Förster Resonance Energy Transfer Effects in Non-Fullerene Ternary Organic Solar Cells with the Third Component Embedded in the Donor and Acceptor. *J Mater. Chem. A* **2017**, 5, 12120-12130.

40. Xu, W.-L.; Wu, B.; Zheng, F.; Yang, X.-Y.; Jin, H.-D.; Zhu, F.; Hao, X.-T., Förster Resonance Energy Transfer and Energy Cascade in Broadband Photodetectors with Ternary Polymer Bulk Heterojunction. *J. Phys. Chem. C* **2015**, 119, 21913-21920.

TOC Graphic